

# A RESOLUTION MEASURE FOR TERRESTRIAL LASER SCANNERS

Derek D. Lichti

Department of Spatial Sciences, Curtin University of Technology, GPO Box U1987, Perth, WA, 6845, Australia –  
[d.lichti@curtin.edu.au](mailto:d.lichti@curtin.edu.au)

Commission V, WG V/1

**KEY WORDS:** LIDAR, Sampling, Resolution, Spatial, Quality, Terrestrial.

## ABSTRACT:

Terrestrial laser scanners are increasingly being used for cultural heritage recording and engineering applications that demand high spatial resolution. Knowledge of an instrument's spatial resolution is necessary in order to prevent aliasing and estimate the level of detail that can be resolved from a scanned point cloud. In the context of laser scanners, spatial resolution can be decoupled into range and angular resolution. The latter is the focus of this paper and is governed primarily by angular sampling interval and laser beamwidth. Both factors give rise to uncertainty in the angular position of a range measurement, though in terms of reporting scanner resolution, it has become a common practise to emphasise one of these factors—typically sampling interval—as an indicator of resolution. Since both affect the resolution of a scanned point cloud, consideration of only one can lead to a misunderstanding of a system's capabilities. The ramification of this is that the actual resolution may be much lower than that perceived when visually inspecting a scan cloud. It will be demonstrated that consideration of only one factor independent of the other is inappropriate except under very specific conditions. A new, more appropriate resolution measure for terrestrial laser scanners is therefore necessary and one is proposed in this paper. The effective instantaneous field of view (EIFOV) is derived by modelling the inherent uncertainties in equal angular increment sampling and laser beamwidth with ensemble average modulation transfer functions (AMTFs). The practical outcome of this approach is a scientifically sound method of quantifying laser scanner resolution for users of the technology. Four commercially available terrestrial laser scanner systems are modelled with AMTFs and analysed in terms of their angular resolution as measured by the EIFOV. It is demonstrated that point cloud resolution as indicated by the EIFOV is much more coarse (by up to 21 times) than the sampling interval.

## 1. INTRODUCTION

Laser scanning instruments are increasingly being used for tasks traditionally performed using photogrammetric and surveying methods. They provide users with a three-dimensional sampled representation—a point cloud—of an object or surface and are used in a diverse range of applications including metrology, as-built surveys, reverse engineering, airborne topographic surveying, cultural heritage recording and volume estimation on mine sites. Though the accuracy requirements for these applications may differ considerably, spatial resolution is an important aspect of any laser scanner survey.

Spatial resolution governs the level of identifiable detail within a scanned point cloud and is particularly important for, say, recording of cultural heritage features with fine details. For laser scanners it can be decoupled into range and angular resolution. Range resolution is the ability of a rangefinder to resolve two objects on the same line of sight (Kamerman, 1993), which is directly proportional to timing resolution for time-of-flight systems (Wehr and Lohr, 1999). Angular resolution, the ability to resolve two objects on adjacent sight lines, is a function of spatial sampling interval and the laser beamwidth. For airborne laser scanner (ALS) systems, the sampling interval is partially dependent upon aircraft motion, whereas scanning mechanisms control it for terrestrial laser scanners (TLSs).

Resolution is a term often abused and misunderstood; emphasis in sales literature tends to be on the finest possible sampling interval, which is often much smaller than the laser beamwidth. Since both factors influence the resolution of a scanned point

cloud, consideration of only one can lead to a misunderstanding of a system's capabilities. To illustrate, consider the article by Iavarone (2002), in which the author states that high scan resolution can be achieved by correlated sampling (i.e. overlapping laser spots) and, therefore, laser beam spot size is not a limiting factor. While this is partially true in the sense that a fine sampling increment yields a high Nyquist frequency, the benefit of correlated sampling is not fully realised because sampling is not the only factor that influences resolution.

A scanned point cloud may *appear* to have very high spatial resolution by virtue of a fine sampling interval and corresponding high point density. The actual spatial resolution may be much lower if the beamwidth is large relative to the sampling interval because the fine details are effectively blurred. It will be demonstrated in this paper that beamwidth can be a significant factor in reducing the spatial resolution of a scan cloud, even in the presence of correlated sampling. Though perhaps not an issue for smooth surfaces, it certainly could be for intricate surfaces with rapidly varying details that might be encountered in cultural heritage recording or as-built surveys of industrial plants.

A new angular resolution measure for laser scanners that models the contributions of both sampling and beamwidth, the effective instantaneous field of view (EIFOV), is proposed. Its need is highlighted with a real dataset example that illustrates positional uncertainty due to beamwidth. The EIFOV is derived from an ensemble average modulation transfer function (AMTF) that models the positional uncertainty due to both factors. Following derivations of the AMTF and EIFOV, the angular resolution of four commercially available terrestrial

laser scanner systems is analysed. Though the analyses focus on terrestrial systems, the AMTF and EIFOV model can also be applied to ALS

## 2. LASER SCANNER RESOLUTION

### 2.1 Sampling interval and beamwidth reporting

Sampling and beamwidth reporting in sales literature varies substantially from one vendor to the next, which can cause confusion about a system's capabilities. To demonstrate, some of the salient properties of four TLS systems are listed in Table 1. The selected scanner vendors use two methods for reporting their *finest* angular sampling interval: spatial interval as a function of range (Optech and Leica) and angular increment (Mensi and Riegl). Note that Leica only provides the interval at one range (50 m), whereas Optech gives a linear function.

Make	Model	Angular Sampling Interval	Laser Beamwidth
Leica	HDS2500	0.25 mm at 50 m	≤ 6 mm from 0 - 50 m
Mensi	GS100	0.0018°	3 mm at 50 m
Optech	ILRIS-3D	0.026R mm, where R is the range to target in m	0.17R+12 mm
Riegl	LMS-Z420i	0.0025°	0.25 mrad divergence

Table 1. Angular sampling interval and beamwidth reporting styles for some commercial TLS systems.

The Optech specifications provide the most descriptive beamwidth information in the form of initial diameter plus linear divergence as a function of range. The Leica beam diameter specification is given for the range 0 – 50 m, while Mensi gives the diameter only at 50 m. Riegl provides the beam divergence, in mrad, that corresponds to the increase in

beam diameter as a function of range. Divergence may also be defined as the linear increase in radius (e.g., Weichel, 1990).

### 2.2 Positional uncertainty due to beamwidth

The inherent positional uncertainty due to beamwidth is highlighted in Figure 1, which depicts a point cloud of a plumb line (2 m long, ≈ 0.1 mm diameter) scanned with a Cyra Cyrax 2500 (now known as the Leica HDS2500) from a range of 5.5 m. Also shown is the estimated plumb line determined by least-squares 3D line fitting. The co-ordinate system is externally defined (i.e. object space) and the X-axis scale has been greatly exaggerated. Several sampling profile lines intersect the plumb line, as indicated by the 2-4 mm long linear bands of points. Angular measurement noise is apparent in the scatter of points about the centreline of each band. The acute angle (approximately 0.4°) between the plumb line and sampling profiles is due to the scanner not being levelled. Levelling is not possible with this instrument.

The band of points along each profile line is due to beamwidth-induced uncertainty in angular position. Its cause is depicted schematically in Figure 2. For each point in this cloud, the range measurement to the backscattering surface (i.e. the plumb line) is made to a point *somewhere* within the projected laser beam footprint. Notwithstanding noise and quantisation effects, the *apparent* angular position of the range measurement is taken by convention to be the centre of the emitted beam. Though a fine feature (such as a plumb line) can be resolved, the actual angular position of the measured point may be biased by up to one-half the beam diameter and cannot be predicted. The position can only be *estimated* with analytical techniques like redundant geometric form fitting. While a plumb line may appear to represent an extreme case, it highlights very well the inherent positional ambiguity due to beamwidth that can exist in all point clouds but may be less obvious upon visual inspection. Beamwidth uncertainty can also manifest itself at edges and tangent to curved objects such as cylindrical pipes. A model that quantifies the uncertainty is proposed in the next section.

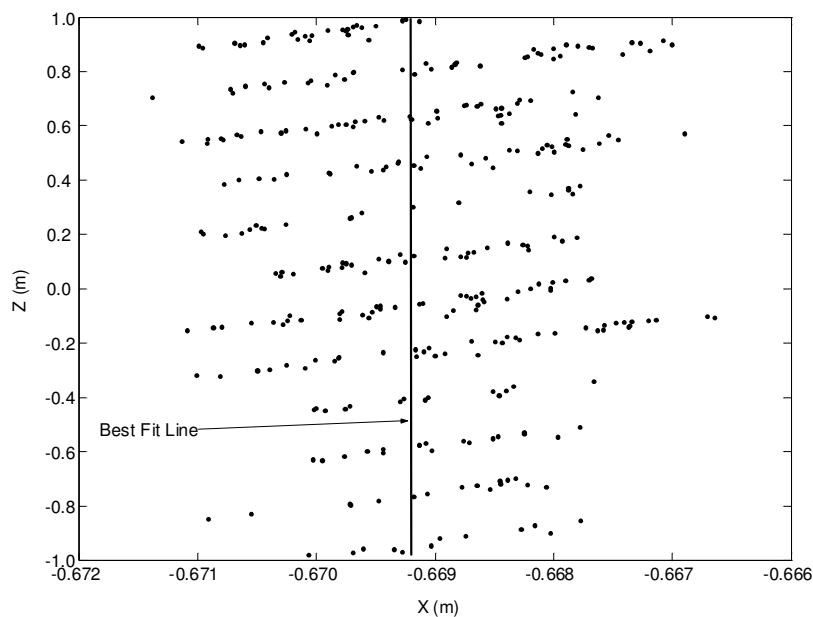


Figure 1. Cyra Cyrax 2500 plumb line point cloud and best fit line.

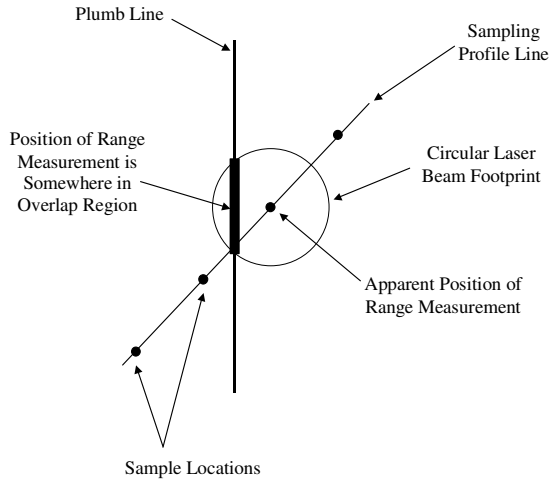


Figure 2. Beamwidth positional uncertainty.

### 3. THE AMTF MODELLING APPROACH

#### 3.1 Equal angular increment sampling

A three-dimensional scan of a scene can be compiled by mechanically deflecting the rangefinder laser beam in equal increments of arc in horizontal and vertical planes. A scanned scene can thus be parameterised in terms of range,  $\rho$ , as a uniformly sampled function of two independent variables: horizontal direction,  $\theta$ , and elevation angle,  $\alpha$ ,

$$\rho_s(\theta, \alpha) = \sum_{m=-\infty}^{\infty} \sum_{n=-\infty}^{\infty} \rho_c(m\Delta, n\Delta) \delta(\theta - m\Delta, \alpha - n\Delta), \quad (1)$$

where  $\rho_s$  is the sampled representation of the continuous scene,  $\rho_c$ , and  $\delta$  in this context represents the Dirac delta function. Note that a single sampling interval,  $\Delta$ , has been assumed for both co-ordinate dimensions.

#### 3.2 Ensemble average functions

The sampled representation of a scene given by Equation 1 is dependent upon the scene phase and, thus, is not shift invariant. To cope with this for digital imaging systems, Park et al. (1984) define the concepts of average system point spread function (PSF) and the average system optical transfer function. The average system PSF is an ensemble average function of randomly located point sources under the assumption that the independent variables are uniformly distributed on the sampling interval (Park et al., 1984). This permits application of modulation transfer function (MTF) analysis—restricted by definition to linear shift-invariant systems—to sampled imaging systems (Boreman, 2001). In this paper, the average MTF concept is applied to model both the sampling process *and* the laser beamwidth in order to derive a measure that accurately quantifies laser scanner angular resolution.

#### 3.3 Scanner sampling AMTF

In the context of laser scanning, the average PSF concept is used to model the ensemble of possible random angular phase

shifts of a scanned scene. Taking the average over one square (i.e.  $\Delta \times \Delta$ ) of the sampling lattice, in which the probability distribution is assumed to be uniform, the resulting sampling average PSF,  $APSF_s$ , is given by:

$$APSF_s(\theta, \alpha) = \begin{cases} \frac{1}{\Delta^2} & |\theta| < \frac{\Delta}{2}; \quad |\alpha| < \frac{\Delta}{2} \\ 0 & \text{otherwise} \end{cases}. \quad (2)$$

The corresponding MTF is given by the modulus of the average PSF's 2D Fourier transform:

$$AMTF_s(\mu, \nu) = \left| \frac{\sin(\pi\Delta\mu)}{\pi\Delta\mu} \frac{\sin(\pi\Delta\nu)}{\pi\Delta\nu} \right|, \quad (3)$$

where  $\mu$  and  $\nu$  are the respective horizontal and vertical (angular) spatial frequency domain variables. Note that although a square sampling lattice has been assumed, the formulation is easily modified to accommodate unequal horizontal and vertical sampling periods or other sampling geometries (e.g., hexagonal). Though the present analysis is restricted to the directions of the co-ordinate axes, ( $\theta$  and  $\alpha$ ;  $\mu$  and  $\nu$ ), attention is drawn to the fact that the resolution measures derived herein are not applicable in other directions due to the angular dependence of  $AMTF_s$  (Hadar et al., 1997).

#### 3.4 Scanner beamwidth AMTF

For the beamwidth resolution model, the probability governing the angular position of a range measurement is assumed to be uniform over the projected laser footprint. Note that this does not refer to the irradiance distribution within the cross-section, which is typically Gaussian. Also, to keep the model generic, a beam diameter definition has not been specified, though the  $e^{-2}$  definition is most common. Integration over a uniform circular region with diameter  $\delta$  yields the beamwidth average PSF,  $APSF_b$ :

$$APSF_b(\theta, \alpha) = \begin{cases} \frac{4}{\pi\delta^2} & \theta^2 + \alpha^2 < \frac{\delta^2}{4} \\ 0 & \text{otherwise} \end{cases}. \quad (4)$$

The corresponding circular beamwidth AMTF is given by:

$$AMTF_b(\mu, \nu) = \left| \frac{2J_1\left(\pi\delta\sqrt{\mu^2 + \nu^2}\right)}{\pi\delta\sqrt{\mu^2 + \nu^2}} \right|, \quad (5)$$

where  $J_1$  is the first order Bessel function of the first kind. Though a circular beam cross-section has been assumed,

average PSFs and MTFs can be derived for other beam shapes (e.g., square, rectangular, elliptical).

### 3.5 Combined AMTF

The physical bases for the sampling and beamwidth AMTFs are analogous to those used to model the sampling and detector footprint effects, respectively, in electro-optical imaging systems (e.g., Boreman, 2001). The product of Equations 3 and 5 gives the combined AMTF for a square sampling lattice and circular beam:

$$AMTF_{sb}(\mu, \nu) = \left| \frac{\sin(\pi\Delta\mu)}{\pi\Delta\mu} \frac{\sin(\pi\Delta\nu)}{\pi\Delta\nu} \frac{2J_1\left(\frac{\pi\delta\sqrt{\mu^2 + \nu^2}}{\pi\delta\sqrt{\mu^2 + \nu^2}}\right)}{\pi\delta\sqrt{\mu^2 + \nu^2}} \right| \quad (6)$$

### 3.6 Laser scanner EIFOV

Numerous measures exist for quantifying the resolution of imaging systems; Holst (1997) gives a comprehensive treatment on the subject. Since spatial domain metrics are often seen as easier to interpret than those in the frequency domain, sampling interval and beamwidth might appear to be appropriate measures for laser scanners. As will be demonstrated, these are appropriate only under very specific conditions.

The effective instantaneous field of view (EIFOV) is favoured for the analysis of electro-optical system resolution because it models all factors that degrade image quality, such as the optics, electronics, etc. (Slater, 1975). The appropriateness of the EIFOV extends to laser scanners because it quantifies the influences of both sampling and beamwidth on resolution. The EIFOV is computed via the cut-off frequency,  $\mu_c$ ,

$$EIFOV = \frac{1}{2\mu_c} \quad (7)$$

at which the AMTF equals a threshold, A, i.e.

$$AMTF_{sb}|_{\mu=\mu_c} = A \quad (8)$$

Note that analysis along the other frequency domain axis,  $\nu$ , is unnecessary since the sampling lattice is square and the beam cross-section shape is circular. Slater (1975) and Park et al. (1984) use  $A = 0.5$ , which was chosen as a compromise between several proposed thresholds. Here,

$$A = \frac{2}{\pi} \approx 0.6366 \quad (9)$$

is proposed to enforce the condition that  $EIFOV = \Delta$  (or, equivalently, the cut-off frequency equals the Nyquist frequency) for  $\Delta \gg \delta$ . This simply reflects the fact that when the sampling interval is very coarse relative to the beamwidth, the main lobe of  $AMTF_b$  is very broad and effectively has unit

amplitude at the cut-off frequency. The cut-off frequency is, therefore, governed solely by  $AMTF_s$ , so a small beamwidth has no influence on angular resolution.

## 4. AMTF ANALYSIS OF TLS SYSTEMS

### 4.1 Resolution analysis

Angular sampling resolution is analysed using the EIFOV measure for the four commercially available TLS systems, all of which can be considered fine resolution scanners in terms of both sampling interval and beamwidth. These are listed along with their pertinent resolution parameters in Table 2. To facilitate the comparison, each vendor's reported *finest* angular sampling interval, beamwidth and calculated EIFOV have been reduced to linear units at a range of 50 m. This is made necessary by the variety of methods vendors use to report resolution information (see Table 1). In all cases a circular laser beam cross-section has been assumed.

Make	Model	$\Delta$ (mm)	$\delta$ (mm)	EIFOV (mm)
Leica	HDS2500	0.25	6.0	5.2
Mensi	GS100	1.6	3.0	3.0
Optech	ILRIS-3D	1.3	20.5	17.7
Riegl	LMS-Z420i	2.2	12.5	10.9

Table 2. Angular resolution measures at 50 m for four commercial TLSs systems.

All four are examples of correlated sampling (i.e.  $\Delta < \delta$ ) in which adjacent samples' projected laser beam footprints overlap. While over-sampling reduces aliasing by increasing the Nyquist frequency, the benefit of doing so is diminished by resolution reduction due to beamwidth. In each case the more realistic EIFOV resolution measure is greater than the sampling interval, by up to 21 times in the case of the Leica HDS2500, 14 times for the Optech ILRIS-3D and 5.0 times for the Riegl LMS-Z420i. The highest resolution instrument, the Mensi GS100, is least influenced by beamwidth ( $EIFOV/\Delta = 1.9$ ) since it has the smallest beamwidth to sampling interval ratio (also 1.9). Note that this instrument does not offer the finest sampling interval and the instrument that does, the Optech ILRIS-3D, has the highest EIFOV and, therefore the lowest resolution.

### 4.2 EIFOV versus sampling interval

Figure 3 shows the EIFOV as a function of sampling interval for each instrument, again in terms of linear units at 50 m to facilitate direct comparison. The left-most endpoints of the curves correspond to  $\Delta$  and EIFOV as reported in Table 2. The curve hierarchy on the EIFOV axis corresponds to the beamwidth, i.e. smaller beamwidth instruments have smaller EIFOVs and, thus, higher angular resolution. The curves have nearly constant trend at small sampling intervals where beamwidth most influences the EIFOV resolution measure. The trend then increases in gradient and eventually converges to the line  $EIFOV = \Delta$  where the influence of beamwidth on resolution is negligible. The convergence rate is inversely proportional to beamwidth. For example, the curves of the Mensi GS100 and Leica HDS2500—instruments with fine beamwidth—converge very rapidly, whereas those with broad

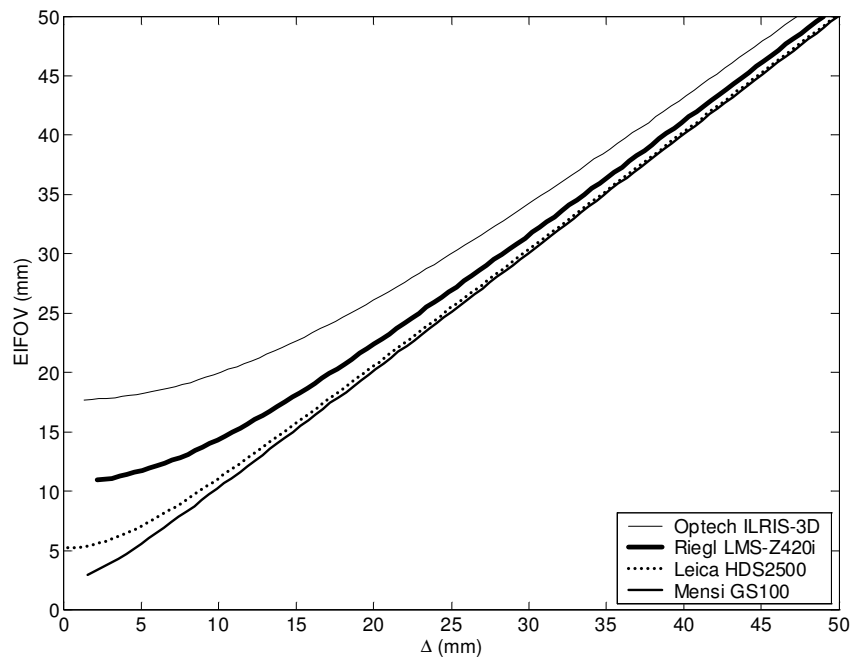


Figure 3. EIFOV vs. sampling interval at 50 m for four TLS systems.

beamwidth, the Riegl LMS-Z420i and Optech ILRIS-3D, converge more slowly. Note also that the EIFOV is never less than the sampling interval under the constraint given by Equation 9.

These analyses demonstrate that neither sampling interval nor beamwidth adequately quantify angular resolution. From Figure 3, it is clear that sampling interval is appropriate only when it equals the EIFOV, i.e. when  $\Delta \gg \delta$ . Beamwidth is equivalent to EIFOV, and thus an appropriate resolution measure, for one multiple of sampling interval:  $\Delta = 0.545\delta$ . This coefficient can be estimated by setting  $\text{EIFOV} = \delta$  and solving Equation 8 for the ratio  $\Delta/\delta$ . The Mensi GS100 happens to satisfy this relationship.

#### 4.3 AMTF analysis

The AMTFs for all four systems' finest sampling interval at 50 m range are plotted along one frequency domain axis in Figure 4 (for positive spatial frequencies only) together with the corresponding cut-off frequencies. Common to all functions is they equal unity at the origin and are non-negative for all frequencies due to the absolute value operation. They decay rapidly to the first zero, beyond which the secondary and higher side lobes have much lower amplitude than the main lobe. Both  $\Delta$  and  $\delta$  govern main lobe width, which is of primary interest, and the locations of the zeroes, whose spacing may not be uniform since Equation 5 is aperiodic in  $\mu$  and  $\nu$ . The resolution hierarchy of the four TLS systems is clearly evident in the main lobe widths and cut-off frequencies shown in Figure 4. For example, the  $\text{AMTF}_{\text{sb}}$  of the highest resolution instrument, the Mensi GS100, has the broadest main lobe and highest cut-off frequency. The narrowest main lobe and lowest cut-off frequency belong to the lowest resolution instrument, the Optech ILRIS-3D.

In the case where sampling interval is much larger than beamwidth (i.e.,  $\Delta \gg \delta$ ), Equation 3 governs AMTF shape (at

low frequencies), since the beamwidth AMTF (Equation 5) has a much greater bandwidth. At the other extreme of  $\Delta \ll \delta$ , the sampling AMTF function has a very broad bandwidth and so the combined AMTF shape resembles Equation 5.

## 5. SUMMARY AND CONCLUSIONS

Both sampling interval and laser beamwidth affect the spatial resolution of laser scanners. The effective instantaneous field of view has been proposed as a more accurate measure of resolution since neither sampling interval nor beamwidth are adequate descriptors except under very specific conditions. To derive the EIFOV, the angular positional uncertainties due to both sampling (i.e., scene phase) and beamwidth have been modelled with ensemble average modulation transfer functions and combined into one AMTF. In essence, the EIFOV is the width of the average point spread function.

Four commercially available terrestrial laser scanner systems have been analysed in terms of their angular resolution capabilities. Perhaps the important result of this process is that a fine angular sampling interval does not necessarily produce a high-resolution point cloud if the beamwidth is significant. Even though a small (in relation to beamwidth) feature can be sensed, its angular position may be biased by up to one-half the beam diameter as indicated by the plumb line example. A fine angular resolution quoted for an instrument should be viewed with scrutiny unless it is much greater than the angular beamwidth because the actual resolution indicated by the EIFOV will be much larger. For example, the ratio of EIFOV to the finest sampling interval reached up to 21 for one of the systems analysed. The benefit of fine sampling interval—higher Nyquist frequency—may not be realised because of the positional uncertainty due to a comparatively large beamwidth. This was confirmed by the TLS system analysis, in which it was found that the highest resolution instrument (in terms of EIFOV) did not possess the finest sampling interval.

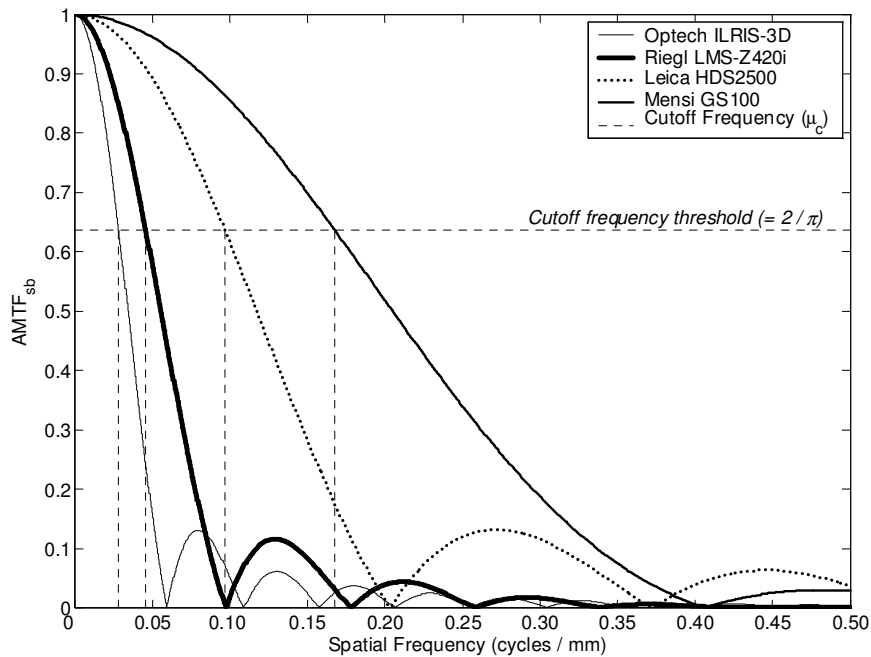


Figure 4.  $AMTF_{sb}$  at 50 m for four TLS systems.

Furthermore, the system offering the finest sampling interval had the largest EIFOV and, therefore, the lowest resolution due to its broad beamwidth.

Some rules of thumb can be derived from the numerical results presented herein. When the sampling interval is much larger than the beamwidth, it is equal to the EIFOV. This is the only condition under which sampling interval accurately represents resolution. When the sampling interval is approximately 55% of the beamwidth, the latter equals the EIFOV, the only condition under which beamwidth accurately describes resolution.

These observations should not be interpreted as criticism of the scanner systems themselves or their inventors. The engineering skill required to develop a working scanning system is indeed impressive. Rather, the message to be gained by readers is that resolution is a function of both sampling interval and beamwidth and, as a result, the attainable resolution of any system will invariably be coarser than is indicated by either of these measures. Thus, the more appropriate EIFOV should be used to measure resolution.

## REFERENCES

- Boreman, G.D., 2001. *Modulation Transfer Function in Optical and Electro-Optical Systems*. SPIE Optical Engineering Press: Bellingham, WA.
- Leica, 2004. [http://www.cyra.com/products/cyrax2500\\_specs.html](http://www.cyra.com/products/cyrax2500_specs.html). Accessed January 29, 2004.
- Hadar, O., A. Dogariu and G.D. Boreman, 1997. Angular dependence of sampling modulation transfer function. *Applied Optics*. 36 (28), 7210-7216.
- Holst, G.C., 1997. *Sampling, Aliasing, and Data Fidelity for Electronic Imaging Systems, Communications, and Data Acquisition*. SPIE Optical Engineering Press: Bellingham, WA.
- Iavarone, A., 2002. Laser scanner fundamentals. *Professional Surveyor* 22 (9). <http://www.profsurv.com/psarchiv.htm>. Accessed January 30, 2004.
- Kammerman, G.W., 1993. Laser radar. In: *Active Electro-Optical Systems*, vol. 6 (C.S. Fox, Ed.). SPIE Optical Engineering Press: Bellingham, WA. pp 1-76.
- Mensi, 2004. <http://www.mensi.com/Website2002/Specs/SpecGS100.pdf>. January 29, 2004.
- Optech, 2004. <http://www.optech.on.ca/>. Accessed January 29, 2004.
- Park, S.K., R. Schowengerdt and M.-A. Kaczynski, 1984. Modulation-transfer-function analysis for sampled image systems. *Applied Optics*. 23 (5), 2572-2582.
- Riegl, 2004. [http://www.riegl.co.at/SSG\\_all.htm](http://www.riegl.co.at/SSG_all.htm). Accessed January 29, 2004.
- Slater, P.N., 1975. Use of MTF in the specification and first-order design of electro-optical and photographic imaging and radiometric systems. *Optica Acta*. 22 (4), 277-290.
- Wehr, A. and U. Lohr, 1999. Airborne laser scanning—an introduction and overview. *ISPRS Journal of Photogrammetry & Remote Sensing* 54(2-3), 68-82.
- Weichel, H., 1990. *Laser Beam Propagation in the Atmosphere*. SPIE Optical Engineering Press: Bellingham, WA.